Effect of Ring-Type Internals on Solids Distribution in a Dual Circulating Fluidized Bed System—Cold Flow Model Study

Diana Carolina Guío-Pérez and Hermann Hofbauer
Division of Chemical Process Engineering and Energy Technology, Institute of Chemical Engineering, Vienna University of Technology, Vienna, Austria

Tobias Pröll
Institute for Chemical and Energy Engineering, Dept. of Material Sciences and Process Engineering, University of Natural Resources and Life Sciences, Vienna, Austria

DOI 10.1002/aic.14120
Published online May 7, 2013 in Wiley Online Library (wileyonlinelibrary.com)

The redistribution of solids in a counter-current circulating fluidized bed (CFB) by effect of ring-type internals was investigated in a downscaled cold-flow model. The system consists of two interconnected CFB reactors, in which the primary reactor operates like a common riser while the secondary reactor operates in counter-current. The unit works without circulation rate control devices and the inventory splits inherently between the two reactors by pressure balance and depending on the fluidization velocities. Previous studies showed an increment in the total pressure drop in the secondary reactor as result of the internals installation. With the purpose of obtaining comparable inventory in the secondary reactor with and without rings, a device for adjustment of total inventory was designed and installed. Effects of the aperture ratio, number of rings, fluidization velocity, and particles circulation rate were studied. The results obtained approach a guideline for the detailed design of similar configurations. © 2013 American Institute of Chemical Engineers *AIChE J*, 59: 3612–3623, 2013

Keywords: fluidization, circulating fluidized beds, internals, particles distribution, counter-current fluidized bed

Introduction and Background

The Dual Circulating Fluidized Bed (DCFB) system and previous work

The dual circulating fluidized bed (DCFB) system under examination was designed for the performance of chemical looping combustion and reforming (CLC and CLR). It consists of two interconnected circulating fluidized beds (CFBs) in which the particles elutriated from the primary reactor (air reactor, AR) are separated in a cyclone and fed to the secondary reactor (fuel reactor, FR) passing through a loop seal. The bed material elutriated from the FR is fed back into the dense zone of this reactor after separation in a cyclone and passing through the corresponding loop seal. The global solids circuit is closed via a loop seal at the lowest end of both the reactors that constitutes a hydraulic connection and permits an inherent stabilization of solids inventories between the two CFBs (Figure 1, left). Both loops work under free circulation principle, that is, the particles' circulation rates are dependent on the fluid dynamics in both the reactors and no control devices for solids circulation are installed. In this particular design, the AR entrainment controls the global solids circulation between the two reactors which in turn determines the transfer rate of heat and chemical species between the reactors. The FR can be independently optimized in order to reach maximum fuel conversion.

In this design, the use of a CFB instead of a bubbling bed as secondary reactor supposes an increment in gas-solids contact compared with other CLC reactor approaches and additionally makes the system suitable for upscaling, as it rules out extremely large inventory requirements.[1] The success on operation of this unit depends principally on two factors: (1) a global solids circulation rate (between AR and FR) should be high enough to satisfy the required oxygen transport and to minimize the temperature difference between the reactors and (2) the gas-solids contact in both reactors should be efficient to ensure good gas conversions.[1–3]

In the FR, a gaseous fuel is used as fluidization medium, the velocity of the fuel determines not only the heat load of the unit but also the fluidization conditions in this reactor. In order to avoid exhaust of unconverted fuel, the fuel velocity needs to be set low enough to provide sufficient residence time to the gas in the reactor, which paradoxically tents to reduce the contact efficiency between phases. In fact, operating experience in the corresponding pilot plant (at the Vienna University of Technology) has shown a need for improvement of the conversion rates in this reactor, it is, need for increasing the contact efficiency and contact time.[1,4] Wedged ring-type internals are proposed to provide this improvement. In previous work, the success of wedged rings in modifying the total hold-up and homogenizing the solids distribution along the reactor was proven.[5] Pressure profiles and corresponding solids

Correspondence concerning this article should be addressed to D. Carolina Guío-Pérez at cguio@mail.zserv.tuwien.ac.at.

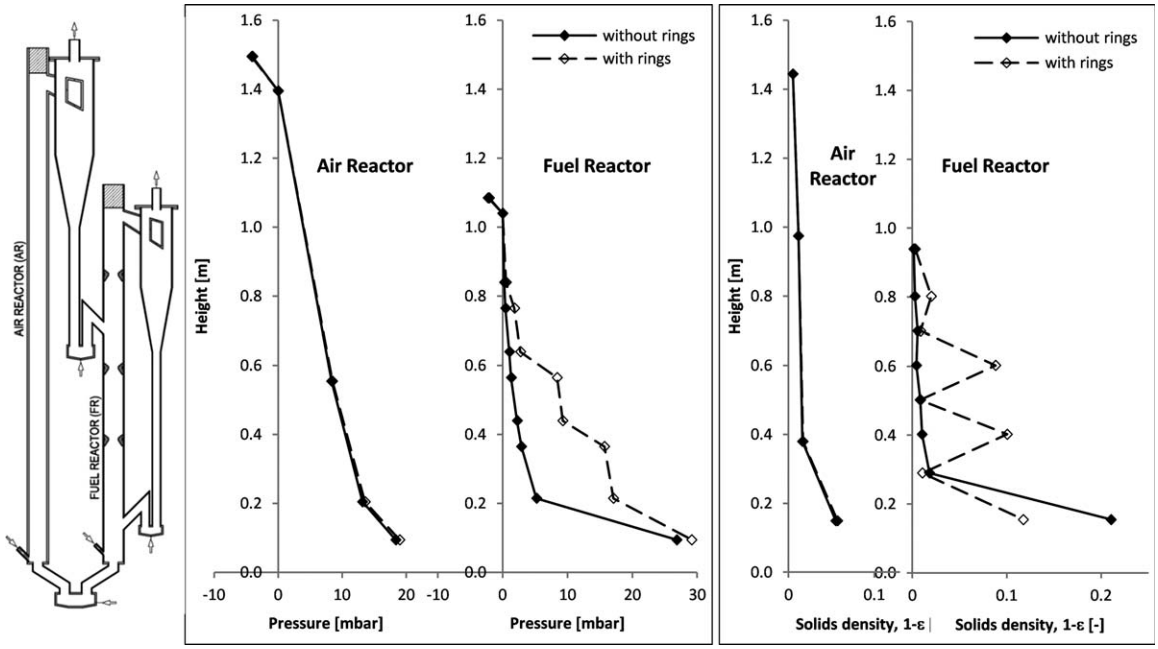

Figure 1. Effect of rings installation, pressure, and solids density profiles in the DCFB system.

Left: Unit scheme. Center: Pressure profiles. Right: Solids density profiles (calculated from the pressure gradients following the relation $(1 - \varepsilon) = (P/(L\Delta pp\Delta g))$.

concentration profiles can be seen in Figure 1 for the system with and without rings, center, and right.

The counter-current and freely circulating nature of the FR makes possible the attainment of a nearly uniformly concentrated structure, not easily reachable in a cocurrent riser. From the first study, it was observed that the wedged rings create a flow pattern comparable to a multistage plates-column where a turbulent contact is reached in each stage, particles concentration becomes in general more evenly distributed along the reactor and particles residence time is probably increased.[6] The formation of consecutive dense regions enables the rise of particles concentration in the upper region of the bed (Figure 1, right). This modification has the advantage of being applicable to high velocity beds, that is, of being able to deal with comparatively larger flows of gas and particles. The absence of drastic constrictions avoids the increase in attrition and pressure drops.

The possibility of providing flexibility to the system, insofar as residence time of gas and solids, contact regime, and velocity of fluidization could be independently controlled to a certain degree, is a key issue for the implementation of this system in a wider spectrum of processes. Applications have been recently proposed by Pröll and Hofbauer[7] and Schmid et al.,[8] which involve operation with diverse type of fuels, that is, diverse particle-size distribution and conversion rates. Schmid et al.[9] have further investigated the changes in regime to be experienced in a counter-current reactor provided with such wedged internals. Other process facing similar requirement regarding gas-solid contact can benefit from installation of wedged rings as well.[10]

Principle of internals implementation—influence on the flow pattern

The modification of the flow structure by means of internals has been studied for decades in slow velocity fluidized beds,[11] some studies have also been completed recently for standard CFBs (a summary can be found in Ref. 12).

Among many different designs, wall baffles in the form of flat rings have been of special interest when it comes to fast fluidized beds; their effects on the gas-solids flow characteristics are well described by Bu and Zhu.[13] Ring-type internals have shown the ability to deflect the particles flowing down at the wall and set them back into the contact-favorable core zone, reducing in this way the typical radial solids concentration nonuniformities and minimizing the solids back-mixing caused by the layer of solids flowing down near the wall.[13,14] The work of Jiang et al.[14] additionally proved an increment of conversion after installation of this kind of internals.

However, when proposing installation of ring-type internals in fast fluidized beds, some practical issues are to be considered[13]: (1) sharp edges are not desirable in order to avoid erosion effects, (2) horizontal surfaces likely promote the accumulation of particles and should be avoided and, and (3) the size of the internals should be carefully revised so that the desired effect of re-entrainment of particles is achieved without creating any important extra resistance to the up-flowing stream.

Addressing these issues, internals in form of wedge-shaped rings were recently proposed.[5] This design is not only suitable for utilization in hot units but also turned out to be successful in avoiding both introduction of extra pressure drop and accumulation of solids. Contrary to the flat rings, the wedge shape eliminates both, the dead zones formed between reactor and rings, and the sharp edges. The re-entrainment and homogenization of particles concentration effects are nevertheless maintained.

After having enunciated the characteristic nonuniformities on particle distributions of the fast fluidized beds and in order to better understand the effect of a wedged obstacle on the flow structure of a CFB, following observations can be made:

1. For the ascending flow of gas, the ring can be seen as a constriction in the pipe. From this point of view, considering a subsonic flow of a gas through a throat under a slight pressure difference, in principle, the pressure undergoes a minimum value at the throat at the same

time that the gas velocity reaches a maximum. A pressure recovery takes place as the gas decelerates.[15] This type of flow can be held to occur with the gas flow that passes through a wedged-ring internal (just when it should meet the descending flow of particles). The inherent pressure drop due to the rings has been demonstrated to be very slight at the operating conditions and type of internals used (Figure 2), that is, a pressure recovery of nearly 100% is reached.

2. A wedge-type internal can be also considered from the point of view of the layer of particles flowing down in the annulus region. Schut et al.[16] reported their observations on the behavior of such annulus layer in a diffuser of a square cross section CFB.[16] The down flow of solids is higher in the diffuser than in the ducts above and below the diffuser, that is, the solids flowing down near the wall tend to form a deposit on the point where the flow direction changes and be projected toward the center (because they are forced to slide down on the slope). Additionally, the upward flow of gas and solids shows signs of separation from the wall in the diffuser. As already indicated by Schut et al. themselves, these findings confirm the re-entrainment of particles from the wall immediately below the diffuser, which due to the geometrical similarity is the phenomenon expected to occur with the installation of wedged rings. The observed separation of the flow from the diffuser wall would also cause recirculation of solids and gas within the diffuser, that is, establishment of strong contact between the phases.
3. Resulting from the convergence of the two previous facts, an acceleration of particles is expected to occur in the vicinity of the internal. In a process similar to the one happening at the bottom of a riser, at the locations right over the rings, the particles and the gas are driven again to get in contact with each other; particles are expected thus to be reaccelerated. This process entails an impulse-transference between the phases, whereby a pressure drop is observed at the positions of installation of rings, and that confirms the re-entrainment. A more precise description of the phenomena taking place at small scale in the vicinity of the rings requires a tighter pressure tapping along the zone concerned. This kind of observations will particularly help when studying on detail the influence of the rings geometry on the desired effects.

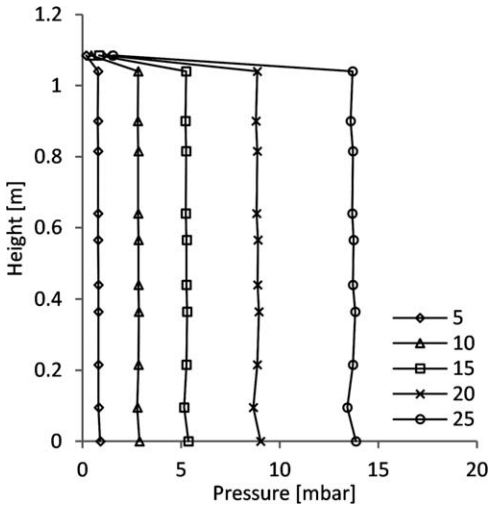

Figure 2. Pressure profile of FR with rings of 60% aperture ratio at different aeration velocities.

No bed material in circulation.

Experimental

Cold model

The experiments for this study were carried out in a cold flow model previously designed and built for the fluid dynamic analysis of a 120 kW chemical looping pilot rig, Figure 3.[17] The model was designed based on Glicksman's

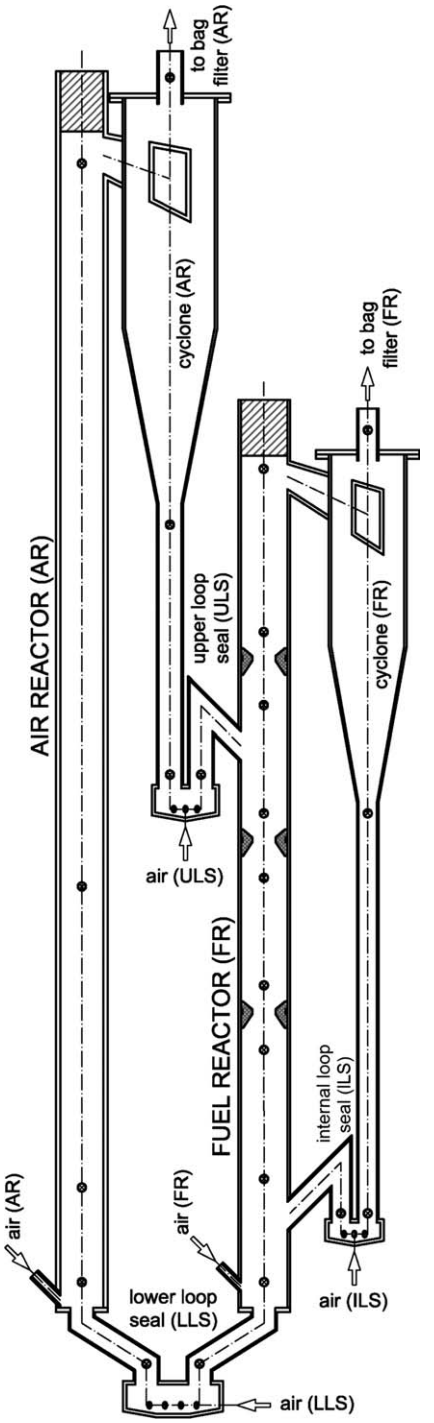

Figure 3. Sketch of the cold flow model including wedged rings.

scaling criteria on a 3:1 scale with respect to the hot unit,[18] the complete set of parameters as presented by Glicksman[18] for the intermediate region (between inertial and viscous limits, $4 > Re_p > 1000$) are considered. These criteria, derived based on the principles of gas-solids flow, are meant to determine the similarity between beds of different size in terms of fluid dynamical behavior. Two units would in principle have identical fluid dynamic behavior when all dimensionless numbers (scaling criteria) are identical. This means that equivalent operation parameters (such as superficial gas velocity) can be simulated in the cold model to obtain corresponding equivalent bed performance parameters (such as riser pressure drop, riser solids hold-up or solids circulation flux).

The fluid-dynamic properties are listed for the materials used in both, hot (H) and cold (C) units and both, AR and FR in Table 1. The design case operation parameters in Table 1 correspond to a 120 kW (fuel power) CLC operation with a global air ratio of 1.2 on the pilot plant using CH4 as fuel. The materials and fluidization conditions in the cold model were selected in order to approximately fulfill the fluid-dynamic similarity. The dimensionless parameters are presented in Table 2 for both, the cold model and the pilot plant. Hot air and hot flue gas are the corresponding gases in the hot unit for the AR and the FR, and an oxygen carrier (metal oxide) with a mean diameter of 161 μm is the bed material. Compressed air was used as fluidization agent in the cold flow model for operational convenience, and spherical bronze powder with a mean diameter of 64 μm was selected as bed material in order to maintain the diameter and density relations (d_P/D and ρ_P/ρ_G as in Table 2).

As it can be seen in Table 2, some compromises are taken regarding the deviations of the different dimensionless groups from the values in the pilot plant. A further decrease of the particle size would decrease the deviation of particle Reynolds number and Archimedes number, however, for such small sizes, interparticle forces are dominant and leads to important electrostatic issues. The importance of wall effect for small reactor diameters and the extent in which the use of small models can produce incorrect results has been usually discussed in literature,[19–21] recommending to avoid cold flow model diameters below 200 mm. In the case of this study, also the diameters of the reactors in the hot unit are below 200 mm. For this work, it was decided to follow a strict linear geometric scaling without additional considerations for wall effects.

The fluidization air flow rates at different positions are controlled using flow meters operated at a constant pressure of 6 bar(abs) followed by manual control valves expanding the gas flows to the operating pressure of the installation, that is, slightly above atmospheric pressure. Pressure was measured along the unit (measurement points indicated in Figure 3) using pressure transducers and a computer to record the pressure values.

The solids circulation has been determined by abruptly stopping the fluidization gas flow in the corresponding loop seal, that is, upper loop seal for global circulation rate and internal loop seal for internal circulation rate,[17] and measuring the time of particle accumulation between defined levels in the cylindrical downcomer after the cyclone. Then the loop seal fluidization continues and the accumulated particles move on. This method is simple to apply but it requires that the mass of particles accumulated in the measurement section is low compared to the total inventory in order not to disturb the system substantially.

The cold flow model is able to simulate fluid dynamical operations conditions corresponding to the hot unit. The particles distribution and the circulation rates can be assumed to be corresponding. Different operating conditions were tested in order to determine the effect of the internals on particles distribution along the reactor as well as on global and internal solids circulation rates.

Wedged ring design

The rings are designed with a wedge shape section that makes them suitable for hot system applications, reduces the possible impact of erosion and avoids inconvenient dead areas above and under the internal. This shape showed good results concerning inherent pressure drop and influence on the flow structure.[5] For this work, two different aperture ratios were tested, 60 and 40% of free area. The precise geometry of the rings can be seen in Figure 4. For each ring type, experiments were performed placing three identical rings in the secondary reactor of the cold flow model at the positions indicated in Figure 3. The whole height of the FR is 1.1 m approximately and the rings were positioned in the heights of 0.4, 0.6, and 0.8 m. An additional experimental series was performed only with the two lower rings in order to identify any potential exit effect caused by the third ring.

Inventory variation

Direct comparison between experiments with and without rings is limited by two factors. On one hand, the total inventory splits inherently between the two reactors by pressure balance and depending on the fluidization velocities in the reactors. On the other hand, installation of wedged rings in the FR likely increases the inventory in this reactor. A solution was sought that enables the adjustment of the total inventory and generates in this manner comparable total pressure drops in the FR for the unit with and without rings.

Table 1. Main Fluid Dynamic Parameters in Hot (H) and Cold (C) Units

Parameter	Dimension	AR_H	FR_H	AR_C	FR_C
η_G	Pa·s	4.70×10^{-5}	4.10×10^{-5}	1.79×10^{-5}	1.79×10^{-5}
ρ_G	kg·m^{-3}	0.316	0.288	1.22	1.22
U	m·s^{-1}	7.32	2.08	4.24	1.21
ρ_P	kg·m^{-3}	3200	3200	8730	8730
d_P	μm	161	161	64	64
Φ	–	0.99	0.99	1.00	1.00
D	mm	150	159	50	54
U_{mf}	m·s^{-1}	0.012	0.015	0.017	0.017
U_t	m·s^{-1}	0.868	1.007	0.909	0.909

Table 2. Comparison of Dimensionless Groups, Hot Installation (H) vs. Cold Flow Model (C)

Parameter	Expression	AR_H	FR_H	AR_C	FR_C	AR_H:AR_C	FR_H:FR_C
Re_P	$\frac{d_P \cdot U \cdot \rho_G \cdot \Phi}{\eta_G}$	7.8	2.3	18.5	5.3	0.42	0.44
Ar	$\frac{\rho_G \cdot (\rho_P - \rho_G) \cdot d_P^3 \cdot g}{\eta_G^2}$	18.7	22.5	85.5	85.5	0.22	0.26
Fr	$\frac{U^2}{g \cdot d_P}$	3.4×10^4	2.7×10^3	2.8×10^4	2.3×10^3	1.18	1.17
Density ratio	$\frac{\rho_P}{\rho_G}$	1.0×10^4	1.1×10^4	7.1×10^3	7.1×10^3	1.42	1.55
Reactor to particle diameter	$\frac{D}{d_P}$	931.7	987.6	781.3	843.8	1.19	1.17

The device designed for such purpose consists of a piston-cylinder system able to contain up to 0.55 kg of bed material. The cylinder was installed in a dense but constantly fluidized zone, namely in the lower loop seal, making possible the introduction or extraction of bed material at any time as long as the loop seal is fluidized. Figure 5 presents the configuration of the inventory variation device.

The inventory was varied in order to obtain a total pressure drop in the FR with rings similar to the one in operation without rings at the corresponding fluidization conditions. That is, to obtain comparable total hold-ups in the FR. The actual inventory in circulation was calculated considering the total inventory initially loaded minus the material lodged in the cylinder for each experiment. The term "total inventory" refers in this work to the amount of material in circulation in the whole unit and should not be confused with the inventory in the FR.

Results and Discussion

For each of the variables studied, pressure profiles and solids density profiles of the FR as well as global and internal circulation rates are presented. Some annotations should be made first in order to get a better understanding of these results:

- It is assumed that the mass (hold up) in the FR is proportional the total pressure drop in this reactor, and hence, the total pressure drop is used to monitor that approximately the same mass is in the reactor for different fluidization conditions.
- As explained, total inventory for the experiments with rings is set in order to match the original total pressure in the FR without internals.
- Neither the rings nor the variation of FR fluidization rate have important influence on the AR as long as the global pressure balance in the unit is maintained[5]; therefore, profiles of the AR are not shown in this article.
- To enable direct comparison of the profiles, pressure drop generated in the cyclones is not considered and the profiles are leveled off to zero at each reactor outlet. The pressure drop in the cyclones is not corresponding to a mass of particles and does not need to be taken into consideration. Therefore, the pressure for the cyclones appears on the negative range of the plots.
- Fluidization velocities (superficial velocities) are calculated from the volumetric flows measured at the corresponding inlet and regarding gas properties and dimensions of each reactor.
- The total mass indicated on the figures corresponds to the actual inventory after subtracting the material lodged in the cylinder; it is to the actual inventory in circulation. Rather than the total inventory, the FR inventory and the circulation rates are considered as independent variables in this study.
- The solids density profiles presented were calculated from the pressure gradients between every two measurement points and following the relation $(1-\varepsilon) = \Delta P / \Delta L \cdot \rho_p \cdot g$. However, this relation is completely valid only if acceleration and buoyancy effects can be neglected. As the system under study does not fulfill completely these premises, the profiles are presented here only as a

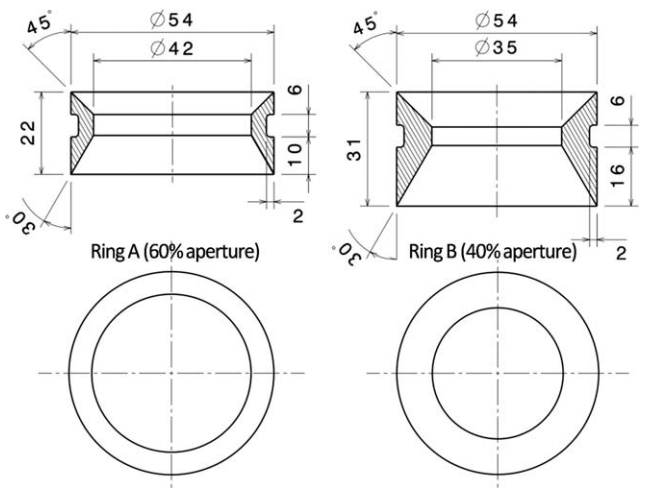

Figure 4. Rings configuration (measures in mm).

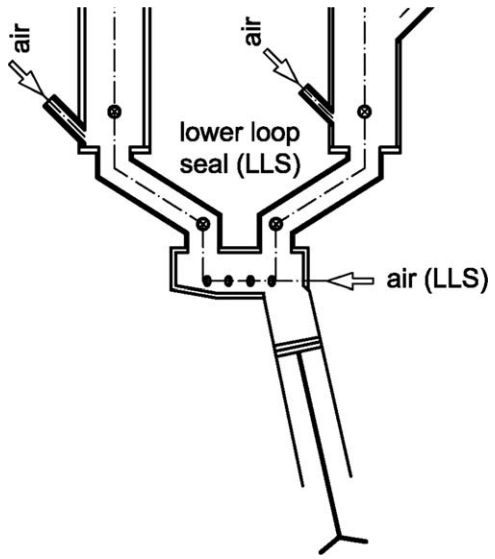

Figure 5. Configuration of the device for inventory variation.

first approach to get an indication of the distribution of solids.

- In order to allow an easy comparison of results for all parameters varied, the results are presented with a similar set of diagrams consisting of: the pressure profiles along the height of the FR, the circulation rates (global and internal) depending on FR or AR fluidization velocity, and the density profiles along the height of the FR.

Bed material redistribution by effect of internals

The influence of the FR fluidization velocity can be observed on the pressure profiles. In Figure 6, a–d, pressure profiles of the FR are compared with and without rings at identical fluidization conditions and varied FR fluidization velocities. As can be seen in Figure 6, e, despite the presence of rings and the fluctuations in inventory, the global circulation rate of solids is kept approximately constant; this makes possible the analysis under the assumption of a similar global circulation rate.

From the solids density profiles the redistribution effect of the rings can be seen, and, furthermore, the dependence of this effect on the fluidization velocity. At low fluidization velocities, where the regime causes a limited bed height, insertion of rings has no influence either on particles distribution or on internal circulation. While at higher gas velocities, which correspondingly generate a higher bed, the presence of the rings becomes an essential factor that significantly influences the axial particles distribution in the reactor. Likewise, the internal circulation is only affected at high

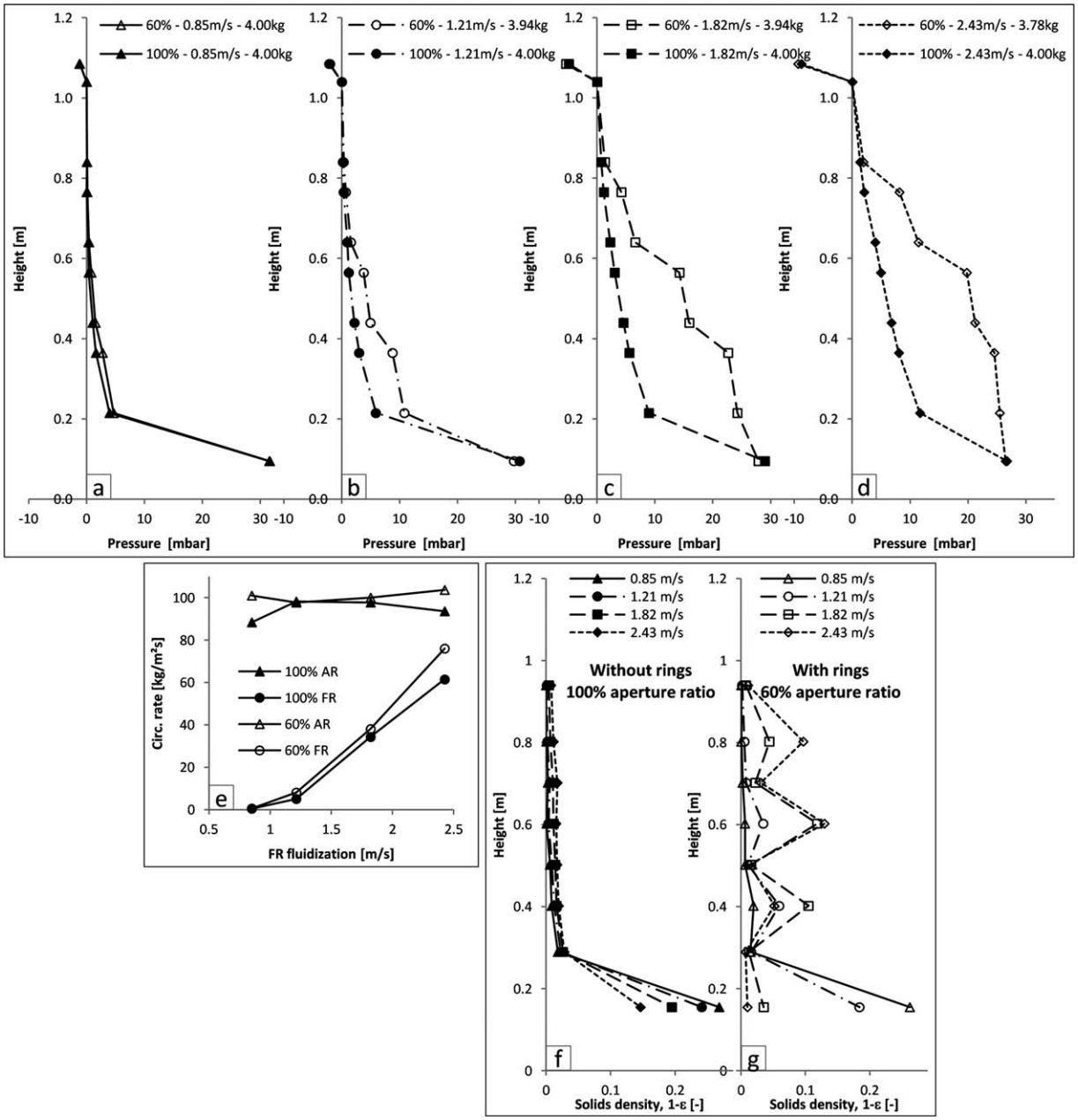

Figure 6. (a–d) Pressure profiles of the FR for different FR fluidizations. (e) Global and internal solids circulation rates. (f–g) Solids density profiles.

Conditions: 4.24 $m \cdot s^{-1}$ of fluidization in the AR. Comparison with three rings type A (60%, empty markers) and without rings (100%, solid markers).

FR fluidization velocities, that is, when the bulk of particles is relocated in the uppermost section of the reactor (Figure 6, e, 1.82 $m \cdot s^{-1}$).

From the results on particles redistribution and internal circulation rate, it can be concluded that two distinguishable zones are created in the FR. The particles entering this reactor between the second and third ring can flow either upwards or downwards depending on the fluidization conditions. The region above the solids inlet can be basically seen as a regular cocurrent fluidized bed, but the section below corresponds to a counter-current reactor. Each of the zones is affected in a different way by the installation of rings. If the height of the bed does not exceed the height of the particles inlet, the particles concentration of the reactor tends to level off without having important influence on circulation rates. But if the bed height goes beyond the solids inlet, elutriation of solids is dominating and leads to a decrease in concentration of particles at the bottom of the reactor and to an important growth of internal circulation rate (decrease in global circulation rate can be observed if the total inventory becomes insufficient).

Without rings, a strong increment of the fluidization velocity is needed in order to enhance the distribution of the particles along the reactor, and even with this only a slight homogenization is reached (see Figure 6, d, 100% aperture ratio, 2.43 $m \cdot s^{-1}$ gas velocity). With the rings, similar particles distribution is reached already with considerably lower fluidization velocity (see Figure 6, b, 60% aperture ratio, 1.21 $m \cdot s^{-1}$ gas velocity). The internal circulation rate of the solids is thereby notably low too. These facts bring out several advantages to the process: (1) high fluidization velocities are not needed, which avoids short gas residence times (that can decrease gas conversion), reduces compression costs and reduces attrition effects and (2), reduction of the solids back-mixing can be expected in as much as the net flow is predominantly downwards and not much material is recirculated in the internal loop. The global particles flow is nevertheless still controlled so that the contact time is enough for the reactions to take place and the solids flow approaches the plug flow structure.

Influence of the global circulation rate and the total inventory

Changes in global circulation rate are generated by varying the AR fluidization velocity (Figure 7, d). Although the circulation rate is dependent on the AR fluidization velocity, the global circulation rate may be considered as an independent variable for the FR.

In general, larger global circulation rates increase the total hold-up in FR and slightly increase the solids concentration as well, but the solids distribution along the reactor remains very similar. Solids distribution is observed to be rather dependent on FR fluidization velocity. Internal circulation rate did not appear to be influenced by the increase of global circulation rate. These results confirm that also with the use of rings, it is possible to optimize conditions in each of the reactors, that is, in each of the reaction zones, in an almost independent way.

As effect of the total inventory increment the global circulation rate is appreciably risen (Figure 8). The internal circulation rate is also increased with the total inventory; however, this increase is significant only at higher FR fluidization velocities (larger than 1,5 $m \cdot s^{-1}$). Internal circulation rates even beyond the maximum manageable by the internal loop seal were reached, which led to blockage of the loop seal and lose of stable operation (the pressure balance cannot be maintained in the internal loop, the loop seal is incapable to keep the recirculation of particles equivalent to the elutriation). Furthermore, this increase in circulation rate entails an increment of the bed height and causes the internals effect to be observed for lower FR fluidizations too. Solids concentration is in general increased in the entire unit with a higher inventory. However, it should be mentioned that the fluidization velocities are still the dominating variables that define the distribution of particles along the reactors (and hence the shape of the pressure profiles).

Influence of the aperture ratio

Two different ring types as presented in the Figure 4 were tested. Figure 9, a–d, compares pressure profiles in the FR for different aperture ratios, 100% (without rings), 60% (rings A), and 40% (rings B). A smaller aperture ratio makes the rings in general more effective in generating an increase in the bed height at low fluidization velocities. It is, for the same fluidization velocity, the smaller the aperture ratio the more particles are located higher in the reactor. This effect leads to a rise of the internal circulation rate, which can become particularly strong at high fluidization velocities (eventually so high that the inventory is insufficient to maintain the global circulation rate).

Smaller aperture ratios appear then more appropriate for applications where the residence time of the gas needs to be prolonged. This is because a low fluidization velocity would already be able to maintain a good distribution of particles in the reactor, together with an enhanced contact regime. These rings will probably increase the residence time of solids in the reactor as well. However, at high fluidization velocities a small aperture ratio would also promote the relocation of the bulk of particles in the uppermost part of the reactor, driving to axial particles distribution nonuniformities (Figure 9, f–g). In other words, the range of fluidization velocities suitable for operation is rather reduced with the use of small aperture ratios.

In contrast, conservative constrictions (larger aperture ratios) do not have important influence at low gas velocity, but are in turn suitable for a broader range of fluidization velocities. They are able to maintain a particles distribution close to the homogeneity at different fluidization conditions and are therefore desirable for processes in which changes in fluidization flow are intended or needed.

Influence of the upper ring

The uppermost ring was removed with the purpose of investigating whether it creates an exit effect in the FR (the two remaining rings were type B, 40% aperture ratio).

Observing Figure 10, it can be said that there are no considerable differences concerning pressure profiles, between the experiments with two and three rings, at the section right over the position of the third ring; this regardless of the fluidization velocity. This indicates the absence of barrier effects on the part of the third ring. However, with increase of fluidization velocity in the FR, an interesting fact is found from the pressure profiles of the region below the third ring. In absence of the last ring, the pressure drop that would be normally shared between second and third rings falls now only on the second one. This is, the fraction of particles that would be located over the third ring is not redistributed along the reactor if the ring is removed, but retained above

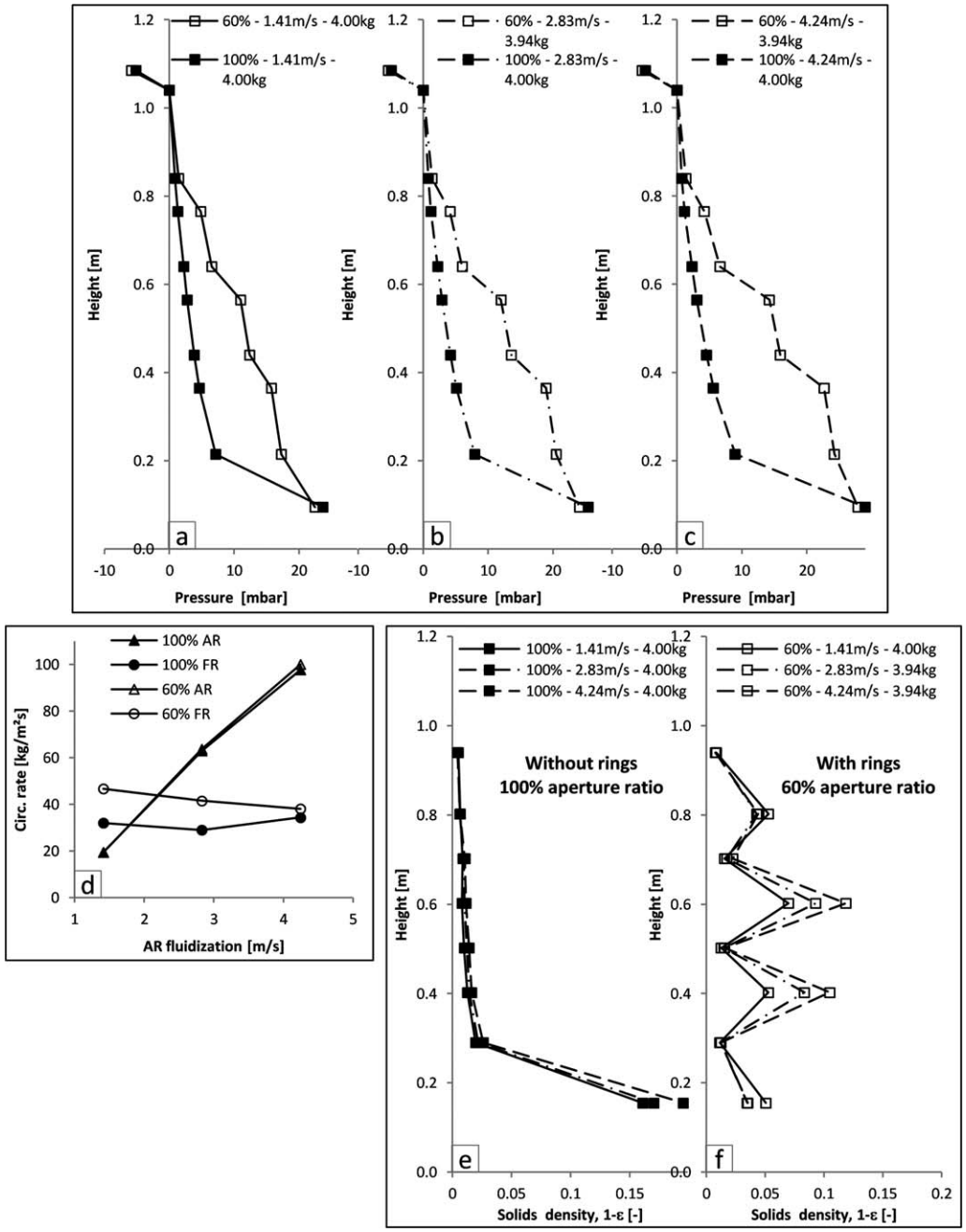

Figure 7. (a–c) Pressure profiles of the FR for different AR fluidizations. (d) Global and internal solids circulation rates. (e–f) Solids density profiles.

Conditions: 1.82 $m \cdot s^{-1}$ of fluidization in the FR. Comparison with three rings type A (60%, empty markers) and without rings (100%, solid markers).

the new uppermost ring. As indicated, this effect is only observed at higher fluidization velocities, at which the bed height should reach the height of the second and third rings (see Figure 10, c–d, 1.82 $m \cdot s^{-1}$, 2,43 $m \cdot s^{-1}$). This effect confirms that the particles carrying capability (set by the fluidization velocity) is ultimately the most determining factor.

Because the internal circulation rate decreased for the experiments in which the bed height would have reached the height of the third ring (experiments at high fluidization velocity), indicates that rather than an obstruction, the third ring has the effect of increasing the net elutriation from the FR toward the cyclone. On this basis, it can be concluded that the absence of the ring in the region above the solids inlet would avoid the increase of the internal circulation rate (considerable at high fluidization velocities), which is undesirable as it disturbs the net downward flow.

Discussion

The particles redistribution effect achieved with the rings is easily observed from the solids concentration profiles. Without rings, particles concentration profile slightly varies, the particles move further up in the column the higher the fluidization rate is, but the exponential shape is preserved, that is, the bulk of particles is kept at the bottom and not much interaction between phases takes place in the upper region of the reactor. On the contrary with rings, variation of fluidization rates strongly modifies the hold-up profiles and

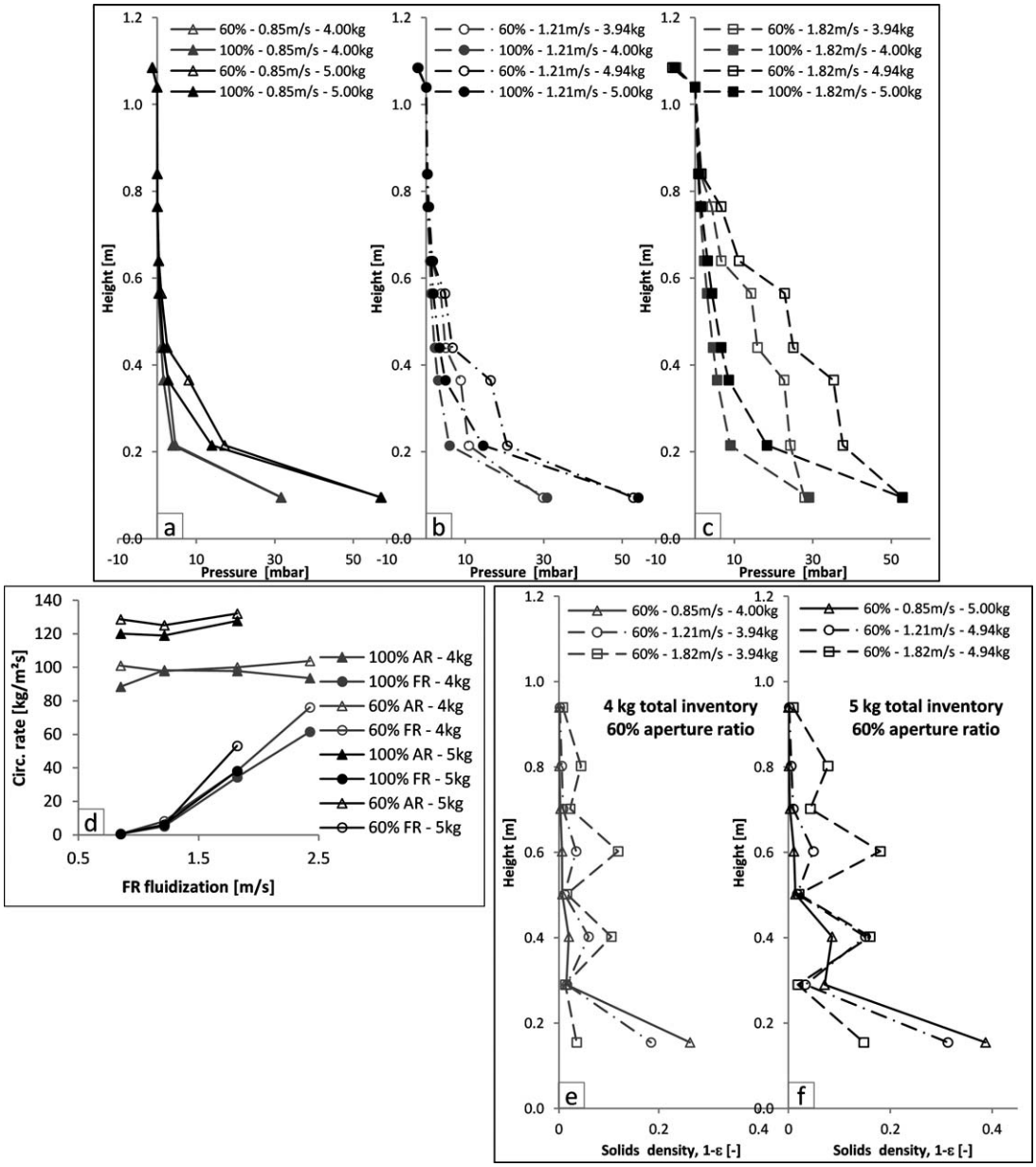

Figure 8. (a–c) Pressure profiles of the FR for different FR fluidizations. (d) Global and internal solids circulation rates. (e–f) Solids density profiles.

Conditions: 4.24 $m \cdot s^{-1}$ of fluidization in the AR, 3 rings type A. Comparison 5 kg total inventory (black markers) and 4 kg total inventory (gray markers).

establishes different states, starting from low-fluidization velocities with most of the particles at the bottom, going through an even distribution of particles among the consecutive sections of the column and ending with most of the particles in the upper section (for high-fluidization rates). Neither the first nor the last state is considered to be optimal. An even distribution is the state aimed to be obtained during operation, as it achieves presence of a good amount of particles along the whole length of the counter-current section of the reactor. This is an extension of the zone of effective gas–solids contact and probably a closer approach to the plug flow structure is achieved.

Then, with the installation of rings higher particles concentration is reached, particularly at high locations in the reactor, without increase in fluidization velocity, which at the same time would minimize the risk of exhausting unconverted fuel and maintains the heat load of the unit. For a given design load (gas power) and inventory requirement, the aperture ratio can be set in order to ensure the optimal particles distribution; in general, the slower the gas velocity is, the more restrictive the constrictions need to be. Nevertheless, a precise design of the reactor will also need to consider following additional aspects:

1. The aperture ratio of the rings will probably have to differ from one another depending on the changes of the volumetric flow rate with the height that occur due to the reactions taking place in the reactor.
2. Taking advantage of the reduction in fluidization velocity that can be implemented after the installation of rings, a reduction in internal circulation rate can be expected. Therefore, the control of the internal loop seal aeration may require special attention in order to avoid fuel bypassing from the reactor toward the cyclone leg (whenever the circulation rate is insufficient to maintain the seal).

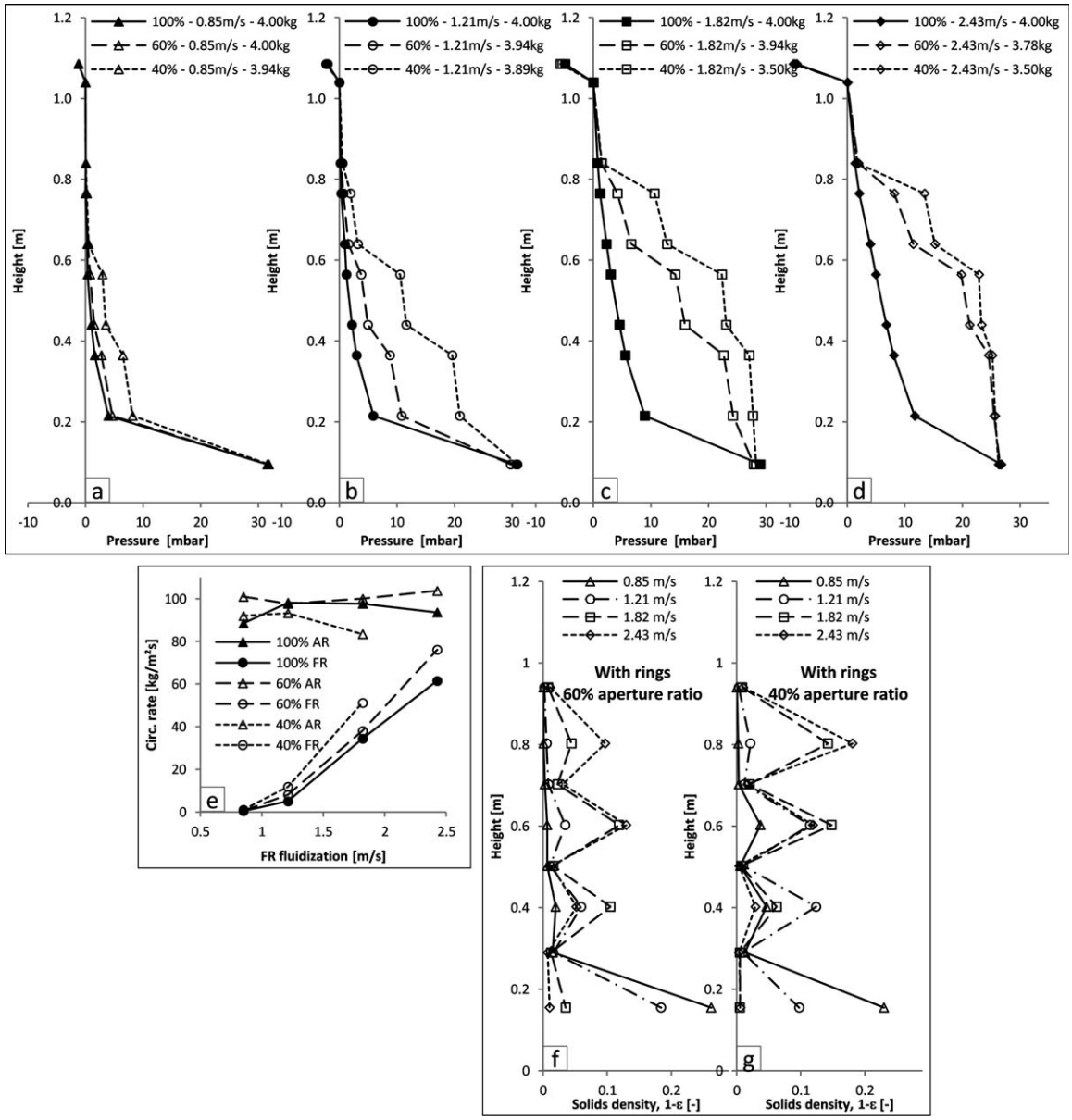

Figure 9. (a–d) Pressure profiles of the FR for different FR fluidizations. (e) Global and internal solids circulation rates. (f–g) Solids density profiles.

Conditions: 4.24 $m \cdot s^{-1}$ of fluidization in the AR. Comparison with three rings type A (60%), three rings type B (40%), and without rings (100%, solid markers).

3. The length of the counter-current section (and the height at which the solids inlet is set), as well as the number of rings in this section are to be defined based on residence time requirements for gas and particles.
4. Installation of rings is not necessarily required at the section above the solids inlet. In fact, because the internal particles circulation rate can be reduce, this section can be shortened.
5. Rings of large aperture ratio can be implemented together with a reactor flue gas recirculation stream, as means to benefit from the effect of rings installation while keeping the load still low.

Conclusions

New progress has been brought to the study of wedged ring-type internals effect on the fluid-dynamic performance of a CFB system for chemical looping. Experimentation in a cold flow model was performed with the implementation of a device able to modify the global inventory. This made possible a precise comparison of pressure profiles under similar hold-up conditions. In this way, the influence of the internals was isolated from the inventory share-out effect, characteristic of the system.

The results suggest that the reactor can be imaginarily divided in to two zones, in each of which rings affect the particles distribution in a different way. Above the inlet of particles, the reactor can be considered as a usual riser, and the rings lead to an increase of internal circulation rate. On the contrary, for the section below the solids inlet, particles and gas flow in counter-current and the rings drive to a homogeneous redistribution of particles that extends the length available for gas-solids contact. Whether the bulk of particles is located above or under the particles inlet, defines the dominating

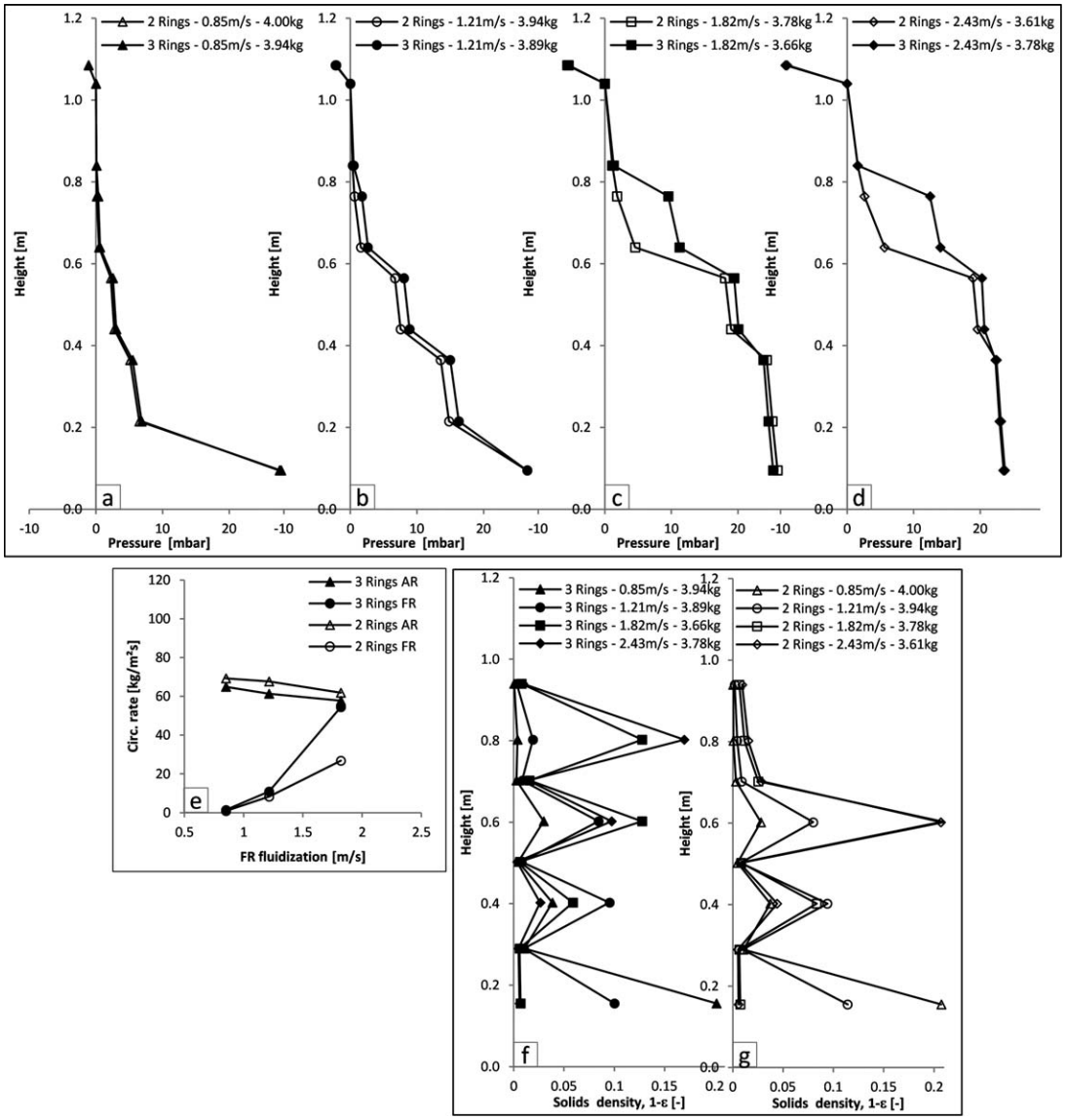

Figure 10. (a–d) Pressure profiles of the FR for different FR fluidizations. (e) Global and internal solids circulation rates. (f–g) Solids density profiles.

Conditions: 2.83 $m \cdot s^{-1}$ of fluidization in the AR. Comparison with two rings type B (60% empty markers) and three rings type B (40% solid markers).

effect. The effect of the rings was consequently found to be strongly dependent on the fluidization velocity of the reactor.

The increment of global circulation influences the total hold-up as well as the concentration of particles in the FR but does not show effect on the distribution of particles. Smaller aperture areas of the rings were found apt to promote the relocation of particles in upper regions already at lower fluidization velocities. However, small aperture ratios reduce the range of fluidization velocities suitable for operation. The ring located above the solids inlet was found to exert the effect of promoting the net elutriation from the FR whenever the bed height reaches the position of the mentioned ring.

After installation of rings, the system still presents its capability for optimization of fluid-dynamic conditions in each of the reactors in an independent way, and additionally introduces the possibility to disengage from one another, velocity of fluidization, regime of the bed, and residence time of gas and particles. This provides the system with even more flexibility for its use under diverse process requirements.

These results present an important improvement in phases contact as well as an increase of residence time of the solids, facts that would derive in both increase of conversion and improvement of heat transfer in the hot unit. Segregation of solids particles is another expectable positive side effect of this design. The verification of these last statements is the goal of ongoing investigations.

Notation

AR = air reactor
Ar = Archimedes number
D = inner riser diameter, m
d_P = mean particle diameter, m
DCFB = dual circulating fluidized bed
FR = fuel reactor
Fr = Froude number
g = gravitational acceleration, $m \cdot s^{-2}$

ILS = internal loop seal
LLS = lower loop seal
Re_P = particle Reynolds number
U = superficial gas velocity, $m \cdot s^{-1}$
U_{mf} = minimum fluidization velocity, $m \cdot s^{-1}$
U_t = terminal fluidization velocity, $m \cdot s^{-1}$
ULS = upper loop seal
$\Delta P/\Delta L$ = pressure gradient, $Pa \cdot m^{-1}$
Φ = mean particle sphericity
η_G = gas dynamic viscosity, $Pa \cdot s$
ρ_G = gas density, $kg \cdot m^{-3}$
ρ_P = particle density, $kg \cdot m^{-3}$
ε = local voidage

Literature Cited

1. Kolbitsch P, Pröll T, Bolhàr-Nordenkampf J, Hofbauer H. Design of a chemical looping combustor using a dual circulating fluidized bed reactor system. *Chem Eng Technol*. 2009;32(3):398–403.
2. Lyngfelt A, Leckner B, Mattisson T. A fluidized-bed combustion process with inherent CO2 separation; Application of chemical-looping combustion. *Chem Eng Sci*. 2001;56:3101–3113.
3. Pröll T, Kolbitsch P, Bolhàr-Nordenkampf J, Hofbauer H. A novel dual circulating fluidized bed system for chemical looping processes. *AIChE J*. 2009;55(12):3255–3266.
4. Pröll T, Mayer K, Bolhar-Nordenkampf J, Kolbitsch P, Mattisson T, Lyngfelt A, Hofbauer H. Natural minerals as oxygen carriers for chemical looping combustion in a dual circulating fluidized bed system. *Energy Procedia*. 2009;1(1):27–34.
5. Guío-Pérez DC, Marx K, Pröll T, Hofbauer H. Fluid dynamic effects of ring-type internals in a dual circulating fluidized bed system. In: Knowlton TM, Editor. *Proceedings of the 10th International Conference on Circulating Fluidized Beds and Fluidization Technology*. New York: Engineering Conferences International, 2011.
6. Toei R, Akao T. Multi-stage fluidised bed apparatus with perforated plates. *IChemE Symp Ser*. 1968;30:34–42.
7. Pröll, T, Hofbauer, H. A dual fluidized bed system for chemical looping combustion of solid fuels. In: *Proceedings of the AIChE Annual Meeting 2010*. Salt Lake City, Utah, 2010.
8. Schmid JC, Pfeifer C, Kitzler H, Pröll T, Hofbauer H. A new dual fluidized bed gasifier design for improved in situ. In: Hofbauer H, Fuchs M. editors. *Proceedings of the International Conference on Polygeneration Strategies 11*. Vienna University of Technology, Vienna, 2011.
9. Schmid JC, Pröll T, Pfeifer C, Rauch R, Hofbauer H. Cold flow model investigation on a modified riser with enhanced gas-solid contact–Locating the regions of operation in a fluidization regime map. In: Proceedings of the 21st International Conference on Fluidized Bed Combustion. Naples, Italy, 2012.
10. Yang W-C, Hoffman J. Exploratory design study on reactor configurations for carbon dioxide capture from conventional power plants employing regenerable solid sorbents. *Ind Eng Chem Res*. 2009;48:341–351.
11. Harrison D, Grace JR. Fluidized bed with internal baffles. In: Davidson JF, Harrison D, Editors. *Fluidization, Chapter 13*. London: Academic Press, 1971:, 599–626.
12. Zhu JX, Salah M, Zhou Y. Radial and axial voidage distributions in circulating fluidized bed with ring-type internals. *J Chem Eng Jpn*. 1997;30(5):928–937.
13. Bu J, Zhu JX. Influence of ring type internals on axial pressure distribution in circulating fluidized bed. *Can J Chem Eng*. 1999;77:26–34.
14. Jiang PJ, Bi HT, Jean RH, Fan LS. Baffle effects on performance of catalytic circulating fluidized bed reactor. *AIChE J*. 1991;37:1392–1400.
15. Holland FA, Bragg R. *Fluid Flow for Chemical Engineers*. London: Edward Arnold Ed., 1994.
16. Schut SB, van der Meer EH, Davidson JF, Thorpe RB. Gas solids flow in the diffuser of a circulating fluidized bed riser. *Powder Technol*. 2000;111:94–103.
17. Pröll T, Rupanovits K, Kolbitsch P, Bolhàr-Nordenkamf J, Hofbauer H. Cold flow model study on a dual circulating fluidized bed system for chemical looping processes. *Chem Eng Technol*. 2009;32(3):418–424.
18. Glicksman L. Scaling relationships for fluidized beds. *Chem Eng Sci*. 1984;39(9):1373–1379.
19. Ellis N, Bi HT, Lim CJ, Grace JR. Hydrodynamics of turbulent fluidized beds of different diameters. *Powder Technol*. 2004;141:124–136.
20. Noymer PD, Hyre MR, Glicksman LR. The effect of bed diameter on near-wall hydrodynamics in scale-model circulating fluidized beds. *Int J Heat Mass Transfer*. 2000;43:3641–3649.
21. Mohanty YK, Roy GK, Biswal KC. Effect of column diameter on dynamics of gas solids fluidized bed: A statistical approach. *Indian J Chem Technol*. 2009;16:17–24.

Manuscript received July 7, 2012, and revision received Mar. 13, 2013.